

Supplementary Information

Effect of Short-Chain Branching on Interfacial Polymer Structure and Dynamics under Shear Flow

Sohdam Jeong,[†] Jun Mo Kim,[†] Soowon Cho, and Chunggi Baig^{*}

*School of Energy and Chemical Engineering, Ulsan National Institute of Science and
Technology (UNIST), UNIST-gil 50, Eonyang-eup, Ulju-gun, Ulsan 689-798, South Korea*

[†]These authors contributed equally to this work.

^{*}Author to whom correspondence should be addressed.

E-mail: cbaig@unist.ac.kr.

Tel: +82-52-217-2538.

Fax: +82-52-217-2649

Materials and Methods

The modified p -SLLOD equations of motion with a Nosé-Hoover thermostat for confined systems have the following expressions:

$$\begin{aligned}\dot{\mathbf{r}}_i &= \frac{\mathbf{p}_i}{m_i} + \mathbf{r}_i \cdot \nabla \mathbf{u}, \\ \dot{\mathbf{p}}_i &= \mathbf{F}_i(\mathbf{r}_i) - \mathbf{p}_i \cdot \nabla \mathbf{u} - m_i \mathbf{r}_i \cdot \nabla \mathbf{u} \cdot \nabla \mathbf{u} - \frac{p_s}{Q} \mathbf{p}_i - \frac{p_s}{Q} (m_i \mathbf{r}_i \cdot \nabla \mathbf{u} - m_i \mathbf{U}(\mathbf{r}_i)),\end{aligned}\quad (1)$$

$$\dot{s} = \frac{p_s}{Q}, \quad \dot{p}_s = F_s(\mathbf{p}_i), \quad Q = DNk_B T \tau_t^2$$

where \mathbf{r}_i , \mathbf{p}_i , and \mathbf{F}_i indicate the position, (nominal) peculiar momentum, and force vector of atom i of the mass m_i . The s and p_s are position-like and momentum-like variables, respectively, of the Nosé-Hoover thermostat. The Q represents the thermostat mass parameter, for which D , N , and τ_t refer the dimensionality of the system, the total number of atoms, and the thermostat relaxation time parameter, respectively. The τ_t was set equal to 0.24 ps in all simulations. The $\nabla \mathbf{u}$, homogeneous velocity gradient tensor, is expressed as

$$\nabla \mathbf{u} = \begin{bmatrix} 0 & 0 & 0 \\ \dot{\gamma} & 0 & 0 \\ 0 & 0 & 0 \end{bmatrix}\quad (2)$$

where $\dot{\gamma}$ is the shear rate. The streaming velocity $\mathbf{U}(\mathbf{r}_i)$ at atomic position \mathbf{r}_i was obtained from a 5th-order polynomial fit in every MD step throughout the total (bulk plus interfacial) region. The real peculiar momentum $\mathbf{p}_i^{\text{real}}$ of each atom was then calculated by removing the streaming velocity at its position from its laboratory momentum $\mathbf{p}_i' = \mathbf{p}_i + m_i \mathbf{r}_i \cdot \nabla \mathbf{u}$:

$$\mathbf{p}_i^{\text{real}} = \mathbf{p}_i' - m_i \mathbf{U}(\mathbf{r}_i)\quad (3)$$

In the TraPPE model, nonbonded atomic interactions including intra-, intermolecular interaction were modeled by a pairwise 6-12 Lennard-Jones (LJ) potential:

$$U_{\text{LJ}}(r_{ij}) = 4\varepsilon_{ij} \left[\left(\frac{\sigma_{ij}}{r_{ij}} \right)^{12} - \left(\frac{\sigma_{ij}}{r_{ij}} \right)^6 \right] \quad (4)$$

where $\varepsilon_{ij} = (\varepsilon_i \varepsilon_j)^{1/2}$ and $\sigma_{ij} = (\sigma_i + \sigma_j) / 2$ were followed the standard Lorentz-Berthelot mixing rules between atomistic units i and j . The LJ parameters σ_{CH} , σ_{CH_2} , and σ_{CH_3} were set equal to 4.68 Å, 3.95 Å, and 3.75 Å, respectively, and the energy parameters $\varepsilon_{\text{CH}}/k_B$, $\varepsilon_{\text{CH}_2}/k_B$, and $\varepsilon_{\text{CH}_3}/k_B$ equal to 10 K, 46 K, and 98 K, respectively. The $r_c = 2.5 \sigma_{ij}$ is a cut-off distance for both atom-atom and atom-wall. In our confined system simulations, wall atoms only interact with fluid atoms, not with each wall atoms. The bonded atomic interactions involving bond-stretching (U_{str}), bond-bending (U_{ben}) and bond-torsional (U_{tor}) were described by

$$U_{\text{str}}(l) = \frac{k_{\text{str}}}{2} (l - l_{\text{eq}})^2, \quad (5)$$

$$U_{\text{ben}}(\theta) = \frac{k_{\text{ben}}}{2} (\theta - \theta_{\text{eq}})^2, \quad (6)$$

$$U_{\text{tor}}(\phi) = \sum_{m=0}^3 a_m (\cos \phi)^m \quad (7)$$

where, for bond-stretching interaction, the bond-stretching constant is $k_{\text{str}}/k_B = 452,900 \text{ K}/\text{Å}^2$ and the equilibrium bond length $l_{\text{eq}} = 1.54 \text{ Å}$. The bond-bending parameter k_{θ} is equal to 122.188 kcal/(mol rad²), and the equilibrium bending angle $\theta_{\text{eq}} = 114^\circ$ for $\text{CH}_x\text{-CH}_2\text{-CH}_y$ (with x and y equal to 2 or 3), $\theta_{\text{eq}} = 112^\circ$ for $\text{CH}_x\text{-CH-CH}_y$, and $\theta_{\text{eq}} = 109.47^\circ$ for $\text{CH}_x\text{-C-CH}_y$. The

bond-torsional parameters are such that (a) $a_0 = 2.0071$, $a_1 = 4.0122$, $a_2 = 0.27105$, $a_3 = -6.2895$ (kcal/mol) for $\text{CH}_x\text{-CH}_2\text{-CH}_2\text{-CH}_y$, (b) $a_0 = 0.78542$, $a_1 = 1.7787$, $a_2 = 0.44454$, $a_3 = -3.5076$ (kcal/mol) for $\text{CH}_x\text{-CH}_2\text{-CH-CH}_y$, and (c) $a_0 = 0.91670$, $a_1 = 2.7503$, $a_2 = 0$, $a_3 = -3.6665$ (kcal/mol) for $\text{CH}_x\text{-CH}_2\text{-C-CH}_y$ [note that here $\phi = 0$ represents the (most stable) *trans*-conformation, whereas it refers to the *cis*-conformation]. The LJ energy and size parameters ϵ and σ are respectively equal to 0.19475 kcal/mol and 3.75 Å for the CH_3 united-atom, 0.09141 kcal/mol and 3.95 Å for the CH_2 united-atom, and 0.01987 kcal/mol and 4.68 Å for the CH united-atom. For bond-bending interaction, the bond-bending constant is $k_{\text{ben}}/k_B = 62,500$ K/rad² and the equilibrium bond angle $\theta_{\text{eq}} = 114^\circ$.

Supplementary Figures

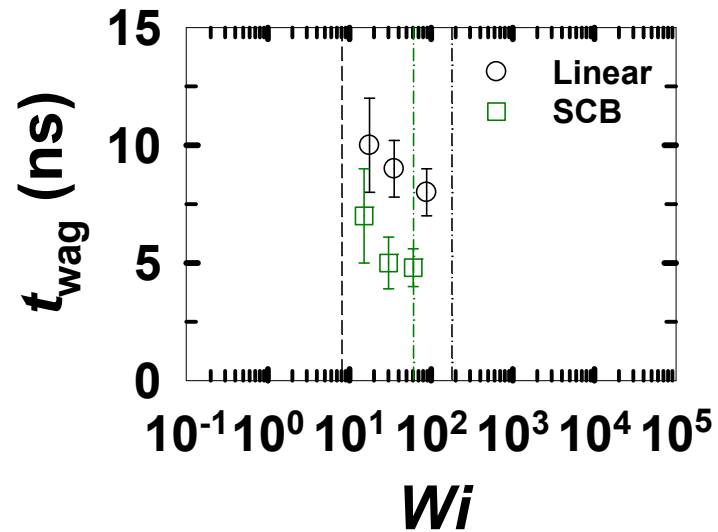


Figure S1. Characteristic time scale (t_{wag}) of the attachment-detachment wagging motions of interfacial chains in the intermediate flow regime for the simulated linear and SCB polyethylene melts, estimated by fitting with a sine function the temporal variations of the average y -position for the center-of-mass of the non-adsorbed parts (y_{nadv}) presented in Fig. 3b in the main text.

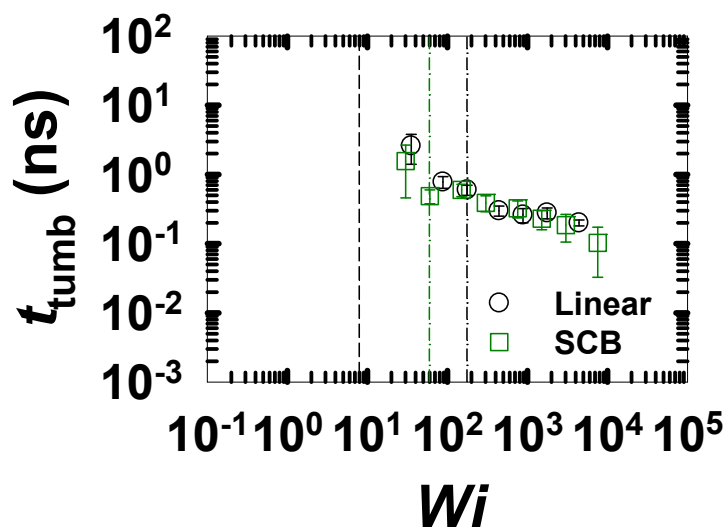


Figure S2. Average tumbling time (t_{tumb}) over all the chains of system for the linear and SCB polyethylene melts as a function of Wi , based on the time correlation function $\langle R_x(t)R_y(0) \rangle$ between the x - and y - components of the chain end-to-end vector \mathbf{R} . We note that due to the frequent movements of the interfacial chains between interfacial and bulk regions in the confined system, it is not feasible to extract the tumbling times only for the interfacial chains. As expected, t_{tumb} decreases with increasing Wi number for both melts. Interestingly, despite that the characteristic rotation and tumbling mechanisms of interfacial chains are different between the two systems (i.e., hairpin tumbling for the linear polymer vs. hairpin tumbling and rolling for the SCB polymer), t_{tumb} is found to be very similar to each other at the same Wi number.

Supplementary Movies

Movie S1: Tumbling dynamics of the interfacial linear polymer

Movie S2: Head-rolling tumbling dynamics of the interfacial SCB polymer

Movie S3: Tail-rolling tumbling dynamics of the interfacial SCB polymer